International Journal of Engineering & Applied Sciences (IJEAS)
Vol.4, Issue 4(2012)41-53

NUMERICAL STUDY ON PULL-IN INSTABILITY ANALYSIS OF GEOMETRICALLY NONLINEAR EULER-BERNOULLI MICRO BEAM BASED ON MODIFIED COUPLE STRESS THEORY

***Y. Tadi Beni* [1], *M. Heidari* [2]**
[1] *Faculty of Engineering, University of Shahrekord, Shahrekord, Iran*
[2] *Mechanical Engineering Group, Aligudarz Branch, Islamic Azad University, Aligudarz, Iran*

Abstract

In this paper, the static pull-in instability of beam-type micro-electromechanical systems (MEMS) is theoretically investigated. Two engineering cases including cantilever and double cantilever micro-beam are considered. Considering the mid-plane stretching as the source of the nonlinearity in the beam behavior, a nonlinear size-dependent Euler-Bernoulli beam model is used based on a modified couple stress theory, capable of capturing the size effect. By selecting a range of geometric parameters such as beam lengths, width, thickness, gaps and size effect, we identify the static pull-in instability voltage. A MAPLE package is employed to solve the nonlinear differential governing equations to obtain the static pull-in instability voltage of microbeams. The results reveal significant influences of size effect and geometric parameters on the static pull-in instability voltage of MEMS.

Keywords: Nonlinear microbeam, modified couple stress theory, static pull-in instability, size effects.

1. Introduction

Micro-electromechanical systems (MEMS) are widely being used in today's technology. So investigating the problems referring to MEMS, owns a great importance. One of the significant fields of study is the stability analysis of the parametrically excited systems. Parametrically excited micro-electromechanical devices are ever increasingly being used in radio, computer and laser engineering [1]. Parametric excitation occur in a wide range of mechanics, due to time dependent excitations, especially periodic ones; some examples are columns made of nonlinear elastic material, beams with a harmonically variable length, parametrically excited pendulums and so forth. Investigating stability analysis on parametrically excited MEM systems is of great importance. In 1995 Gasparini et al. [2] studied on the transition between the stability and instability of a cantilevered beam exposed to a partially follower load. Applying voltage difference between an electrode and ground causes the electrode to deflect towards the ground. At a critical voltage, which is known as pull-in voltage, the electrode becomes unstable and pulls-in onto the substrate. The pull-in behavior of MEMS actuators has been studied for over two decades without considering the casimir force [3–5]. Osterberg et al. [3, 4] investigated the pull-in parameters of the beam-type and circular MEMS actuators using the distributed parameter models. Sadeghian et al. [5] applied the generalized differential quadrature method to investigate the pull-in phenomena of micro-switches. A comprehensive literature review on investigating MEMS actuators can be found in Ref. [6]. Further information about modeling pull-in instability of MEMS has been presented in Ref. [7, 8]. The classical continuum mechanics theories are not capable of prediction and explanation of the size-dependent behaviors which occur in micron- and sub-micron-scale structures. However, some non-classical continuum theories such as higher-order gradient theories and the couple stress theory have been developed such that they are acceptably able to interpret the size-dependencies.

In 1960s some researchers such as Koiter [9], Mindlin [10] and Toupin [11] introduced the couple stress elasticity theory as a nonclassic theory capable to predict the size effects with appearance of two higher-order material constants in the corresponding constitutive equations. In this theory, beside the classical stress components acting on elements of materials, the couple stress components, as higher-order stresses, are also available which tend to rotate the elements. Utilizing the couple stress theory, some researchers investigated the size effects in some problems [12].Employing the equilibrium equation of moments of couples beside the classical equilibrium equations of forces and moments of forces, a modified couple stress theory introduced by Yang, Chong, Lam, and Tong [13], with one higher-order material constant in the constitutive equations. Recently, size-dependent nonlinear Euler–Bernoulli and Timoshenko beams modeled on the basis of the modified couple stress theory have been developed by Xia et al. [14], and Asghari et al. [15], respectively. Rong et al. [16] present an analytical method for pull-in analysis of clamped–clamped multilayer beam. Their method is Rayleigh-Ritz method and assumes one deflection shape function. They derive the two governing equations by enforcing the pull-in conditions that the first and second order derivatives of the system energy functional are zero. In their model, the pull-in voltage and displacement are coupled in the two governing equations.

This paper investigates the pull-in instability of micro-beams with a curved ground electrode under action of electric field force within the framework of von-Karman nonlinearity and the Euler–Bernoulli beam theory. The static pull-in voltage instability of clamped-clamped and cantilever micro-beam are obtained by using MAPLE commercial software. The effects of geometric parameters such as beam lengths, width, thickness, gaps and size effect are discussed in detail through a numerical study. To the authors' best knowledge, no previous studies which cover all these issues are available.

2. Preliminaries

In the modified couple stress theory, the strain energy density $\bar{u}$ for a linear elastic isotropic material in infinitesimal deformation is written as [17]:

$$\bar{u} = \frac{1}{2}(\sigma_{ij}\varepsilon_{ij} + m_{ij}\chi_{ij}) \quad (i, j = 1,2,3) \tag{1}$$

Where

$$\sigma_{ij} = \lambda\varepsilon_{mm}\delta_{ij} + 2\mu\varepsilon_{ij} \tag{2}$$

$$\varepsilon_{ij} = \frac{1}{2}((\nabla u)_{ij} + (\nabla u)_{ij}^{T}) \tag{3}$$

$$m_{ij} = 2l^{2}\mu\chi_{ij} \tag{4}$$

$$\chi_{ij} = \frac{1}{2}((\nabla\theta)_{ij} + (\nabla\theta)_{ij}^{T}) \tag{5}$$

In which σ_{ij}, ε_{ij}, m_{ij} and χ_{ij} denote the components of the symmetric part of stress tensor σ, the strain tensor ε, the deviatoric part of the couple stress tensor m and the symmetric part of the curvature tensor χ, respectively. Also, u and θ are the displacement vector and the rotation vector. The two Lame constants and the material length scale parameter are represented by λ, μ and l, respectively. The Lame constants are written in terms of the Young's modulus E and the Poisson's ratio ν as $\lambda = \nu E/(1+\nu)(1-2\nu)$ and $\mu = E/2(1+\nu)$. The components of the infinitesimal rotation vector θ_i are related to the components of the displacement vector field u_i as [18]:

$$\theta_i = \frac{1}{2}(curl(u))_i \tag{6}$$

For an Euler–Bernoulli beam, the displacement field can be expressed as:

$$u_x = u(x,t) - z\frac{\partial w(x,t)}{\partial x},\ u_y = 0,\ u_z = w(x,t) \tag{7}$$

Where u is the axial displacement of the centroid of sections, and w denotes the lateral deflection of the beam. The parameter $\partial w/\partial x$ stands for the angle of rotation (about the y-axis) of the beam cross-sections. Assuming the above displacement field, after deformation, the cross sections remain plane and always perpendicular to the center line, without any change in their shapes. It is noted that parameter z represents the distance of a point on the section with respect the axis parallel to y-direction passing through the centroid.

3. Governing Equation of Motion

In this section, the governing equation and corresponding classical and non-classical boundary conditions of a nonlinear microbeam modeled on the basis of the couple stress theory are derived. The coordinate system and loading of an Euler–Bernoulli beam have been depicted in Fig. 1. In this figure, *F(x,t)* and *G(x,t)* refer to the intensity of the transverse distributed force and the axial body force, respectively, both as force per unit length.

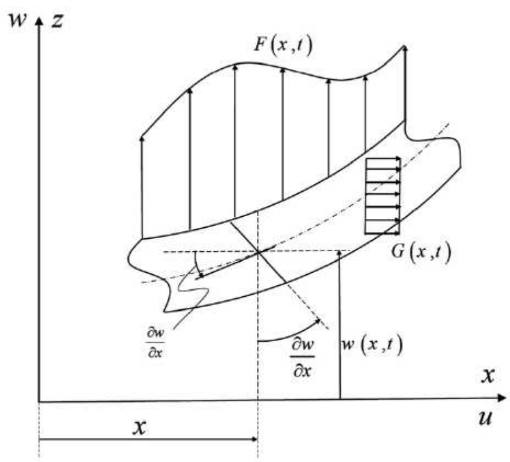

Fig. 1. An Euler–Bernoulli, loading and coordinate system.

By assuming small slopes in the beam after deformation, the axial strain, i.e. the ratio of the elongation of a material line element initially in the axial direction to its initial length, can be approximately expressed by the von-Karman strain as:

$$\varepsilon_{xx} = \frac{\partial u_x}{\partial x} + \frac{1}{2}\left(\frac{\partial w}{\partial x}\right)^2 = \frac{\partial u}{\partial x} - z\frac{\partial^2 w}{\partial x^2} + \frac{1}{2}\left(\frac{\partial w}{\partial x}\right)^2 \tag{8}$$

It is noted that finite deflection w is permissible and only it is needed that the slopes be very small. Hereafter, we use Eq. (8) for the axial strain, instead of the infinitesimal definition presented in Eq. (3). Substitution of Eqs. (7) and (8) into (3)–(5) yields the non-zero components. Also, combination of Eqs. (6) and (7) gives [19]:

$$\theta_y = -\frac{\partial w}{\partial x}, \theta_x = \theta_z = 0 \tag{9}$$

Substitution of Eq. (9) into (5) yields the following expression for the only non-zero components of the symmetric curvature tensor:

$$\chi_{xy} = \chi_{yx} = -\frac{1}{2}\frac{\partial^2 w}{\partial x^2} \tag{10}$$

It is assumed that the components of strains, rotations and their gradients are sufficiently small. By neglecting the Poisson's effect, substitution of Eq. (8) into Eq. (2) gives the following expressions for the main components of the symmetric part of the stress tensor in terms of the kinematic parameters:

$$\sigma_{xx} = E\varepsilon_{xx} = E\left(\frac{\partial u}{\partial x} - z\frac{\partial^2 w}{\partial x^2} + \frac{1}{2}\left(\frac{\partial w}{\partial x}\right)^2\right), \text{ all other } \sigma_{ij} = 0 \tag{11}$$

Where E denotes the elastic modulus. In order to write the non-zero components of the deviatoric part of the couple stress tensor in terms of the kinematic parameters, one can substitute Eq. (10) into Eq. (4) to get:

$$m_{xy} = -\mu l^2 \frac{\partial^2 w}{\partial x^2} \tag{12}$$

Where μ and l are shear modulus and the material length scale parameter, respectively.

To obtain the governing equations, the kinetic energy of the beam T, the beam strain energy due to bending and the change of the stretch with respect to the initial configuration U_{bs}, and the increase in the stored energy with respect to the initial configuration due to the existence of initially axial load U_{is} and finally the total potential energy $U = U_{bs} + U_{is}$ are considered as follows:

$$T = \frac{1}{2}\int_0^L\int_A \rho\left\{\left(\frac{\partial u}{\partial t} - z\frac{\partial^2 w}{\partial t \partial x}\right)^2 + \left(\frac{\partial w}{\partial t}\right)^2\right\} dA\, dx \tag{13a}$$

$$U = \frac{1}{2}\int_0^L \left\{EI\left(\frac{\partial^2 w}{\partial x^2}\right)^2 + EA\left(\frac{\partial u}{\partial x} + \frac{1}{2}\left(\frac{\partial w}{\partial x}\right)^2\right)^2 + N_0\left[2\frac{\partial u}{\partial x} + \left(\frac{\partial w}{\partial x}\right)^2\right] + \frac{\mu A l^2}{2}\left(\frac{\partial^2 w}{\partial x^2}\right)\right\} dx \tag{13b}$$

Where N_0, I and ρ are the axial load, area moment of inertia of section about y– axis and the mass density, respectively. The work done by the external loads acting on the beam is also expressed as:

$$\delta W=\int_0^L F(x,t)\delta w\,dx+\int_0^L G(x,t)\,\delta u\,dx+(\hat{N}\,\delta u)\Big|_{x=0}^{x=L}+(\hat{V}\,\delta w)\Big|_{x=0}^{x=L}+(\hat{M}\,\delta(\frac{\partial w}{\partial x}))\Big|_{x=0}^{x=L}$$
$$+(\hat{P}^h\,\delta(\frac{\partial u}{\partial x}+\frac{1}{2}(\frac{\partial w}{\partial x})^2)\Big|_{x=0}^{x=L}+(\hat{Q}^h\,\delta(\frac{\partial^2 w}{\partial x^2}))\Big|_{x=0}^{x=L} \quad (13c)$$

Where $\hat{N}$ and $\hat{V}$ represent the resultant axial and transverse forces in a section caused by the classical stress components acting on the section. The resultant axial and transverse forces are work conjugate to u and w, respectively. Also, $\hat{P}^h$ and $\hat{Q}^h$ are the higher-order resultants in a section, caused by higher-order stresses acting on the section. These two higher-order resultants are work conjugate to $\varepsilon_{xx}=\partial u/\partial x+1/2(\partial w/\partial x)^2$ and $\partial^2 w/\partial x^2$, respectively. The parameter $\hat{M}$ is the resultant moment in a section caused by the classical and higher-order stress components. Now, the Hamilton principle can be applied to determine the governing equation:

$$\int_{t_1}^{t_2}(\delta T-\delta U+\delta W)dt=0 \quad (14)$$

Where δ denotes the variation symbol. By applying Eqs. 13 and 14, the governing equilibrium micro beam is derived as:

$$S\frac{\partial^4 w}{\partial x^4}-N\frac{\partial^2 w}{\partial x^2}+\rho A\frac{\partial^2 w}{\partial t^2}=F(x,t) \quad (15)$$

Where

$$N=N_0+\frac{EA}{2L}\int_0^L(\frac{\partial w}{\partial x})^2 dx \quad (16)$$

$$S=EI+\mu A l^2 \quad (17)$$

If in Eq. (15) , $N=0$, then the model of beam is called the linear equation without the effect of geometric nonlinearity. The cross sectional area and length of beam are A and L respectively. $F(x,t)$ is the electrostatic force per unit length of the beam. The electrostatic force enhanced with first order fringing correction can be presented in the following equation [20]:

$$F_{elec}(x,t)=\frac{\varepsilon_0 B V^2}{2(g-w)^2}[1+0.65\frac{(g-w)}{B}] \quad (18)$$

Where $\varepsilon_0=8.854\times10^{-12}\,C^2N^{-1}m^{-2}$ is the permittivity of vacuum, V is the applied voltage, g is the initial gap between the movable and the ground electrode and B is width of beam. For clamped-clamped beam, the boundary conditions at the ends are:

$$w(0)=0,\ \ \frac{dw(0)}{dx}=0;\ \ w(L)=0,\ \ \frac{dw(L)}{dx}=0 \quad (19)$$

For cantilever beam, the boundary conditions at the ends are:

$$w(0)=0,\ \ \frac{dw(0)}{dx}=0;\ \ \frac{d^2w(L)}{dx^2}=0,\ \ \frac{d^3w(L)}{dx^3}=0 \quad (20)$$

Table 1. Geometrical parameters and material properties of micro-beam.

Material properties		Geometrical dimensions			
E(GPa)	ν	$L\,(\mu m)$	$B\,(\mu m)$	$h\,(\mu m)$	$g\,(\mu m)$
77	0.33	100-500	0.5-50	0.5-4	0-30

In the static case, we have $\frac{\partial}{\partial \tau}=0$ and $\frac{\partial}{\partial x}=\frac{d}{dx}$. Hence, Eq. (15) is reduced to:

$$(EI+\mu Al^2)\frac{d^4w}{dx^4}-[N_0+\frac{EA}{2L}\int_0^L(\frac{dw}{dx})^2dx]\frac{d^2w}{dx^2}=\frac{\varepsilon_0 BV^2}{2(g-w)^2}[1+0.65\frac{(g-w)}{B}] \qquad (21)$$

A uniform microbeam has a rectangular cross section with height *h* and width *B*, subjected to a given electrostatic force per unit length. Let us consider the following dimensionless parameters:

$$\alpha=\frac{AL^2}{2I},\ \beta=\frac{\varepsilon_0 BV^2L^4}{2g^3EI},\ \gamma=0.65\frac{g}{B},\ \delta=\frac{\mu Al^2}{EI},\ \tilde{w}=\frac{w}{g},\ \tilde{x}=\frac{x}{L},\ \Gamma=\frac{N_0L^2}{EI} \qquad (22)$$

In the above equations, the non-dimensional parameter, δ is defined the size effect parameter. Also, β is non-dimensional voltage parameter. The normalized nonlinear governing equation of motion of the beam can be written as [21]:

$$(1+\delta)\frac{d^4\tilde{w}}{d\tilde{x}}-\{\Gamma+\alpha\int_0^1(\frac{d\tilde{w}}{d\tilde{x}})^2\,d\tilde{x}\}\frac{d^2\tilde{w}}{d\tilde{x}^2}=\frac{\beta}{(1-\tilde{w})^2}+\frac{\gamma\beta}{(1-\tilde{w})} \qquad (23)$$

4. Results and Discussion

4.1. Static pull-in instability analysis

When the applied voltage between the two electrodes increases beyond a critical value, the electric field force cannot be balanced by the elastic restoring force of the movable electrode and the system collapses onto the ground electrode. The voltage and deflection at this state are known as the pull-in voltage and pull-in deflection, which are of utmost importance in the design of MEMS devices. The pull-in voltage of cantilever and fixed-fixed beams is an important variable for analysis and design of micro-switches and other micro-devices. Typically, the pull-in voltage is a function of geometry variable such as length, width, and thickness of the beam and the gap between the beam and ground plane. To study the instability of the nano-actuator, Eq. (23) is solved numerically and simulated. To highlight the differences between linear and nonlinear geometry model results of Euler-Bernoulli microbeam, we first compare the pull-in voltage for a fixed-fixed and cantilever beams with a length of $100\,\mu m$, a width of $50\,\mu m$, a thickness of $1\,\mu m$ and two gap lengths. For a small gap length of $0.5\,\mu m$ (shown in Fig. 2), we observe that linear and nonlinear geometry model give identical results. However, for a large gap length of 2 μm (shown in Fig. 3), we observe that pull-in voltage for fixed-fixed beam is significantly different. As shown in Fig. 4, the difference in the pull-in voltage is even larger when a gap length of $4.5\,\mu m$ is considered. In figures 5, 6 and 7, pull-in voltage of fixed-free beams are shown. It is evident that pull-in voltage of fixed-fixed beam is larger than fixed-free beam. More extensive studies for the cantilever beam with lengths varying from 100 to $500\,\mu m$ and thicknesses varying from 1 to $4\,\mu m$ are shown in Figs. 8 and 9. The gap lengths used vary from 5 to $30\,\mu m$. For gaps smaller than $15\,\mu m$ and lengths larger than $350\,\mu m$, we observe that the pull-in voltage obtained with linear and nonlinear geometry model are very close. However, for large gaps (such as the 15 μm case) and for short beams (such as the 100 μm case), we observe that the difference in the pull-in voltage obtained with linear and nonlinear geometry model is not negligible. In Figs. 10-11, we investigate the fixed-fixed beam example with lengths varying from 100 to 500 μm and thickness varying from 0.5 to 2 μm . We observe that, for all cases, the pull-in voltage obtained with linear model are in significant error (larger than 5.5%) compared to the pull-in voltages obtained with nonlinear geometry model. When the gap increase, the error in pull-in voltage with linear model increase significantly. Furthermore, contrary to the case of cantilever beams, the thickness has a significant effect on the error in pull-in voltages. The thinner the beam, the larger the error. Another observation is that the length of the beam has little effect on the error in pull-in voltage. This observation is also different from the case of cantilever beams. From the results, it is clear the linear model is generally not valid for the fixed-fixed beams case, except when the gap is very small, such as the 0.5 μm case as shown in Fig. 2. Effect of the size effect on the pull-in voltage of fixed-fixed and fixed-free beam illustrated in Figs. 12 and 13 respectively. These figures represent that the size effect increases the pull-in voltage of the nano-actuators.

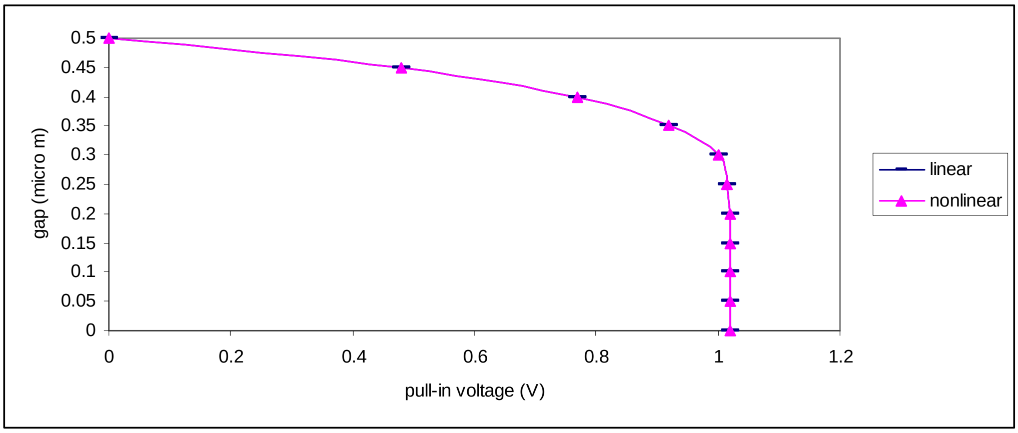

Fig.2. Comparison of linear and nonlinear geometry model results for a fixed-fixed beam with a gap 0.5 μm

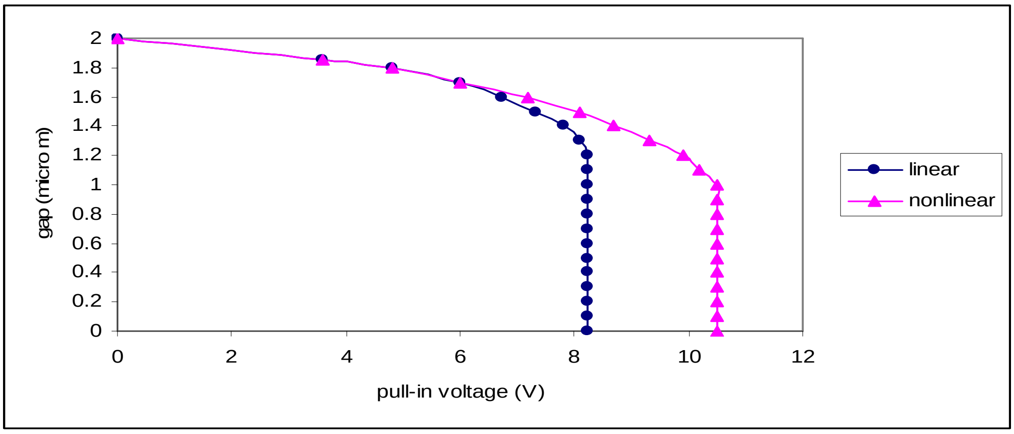

Fig.3. Comparison of linear and nonlinear geometry model results for a fixed-fixed beam with a gap 2 μm

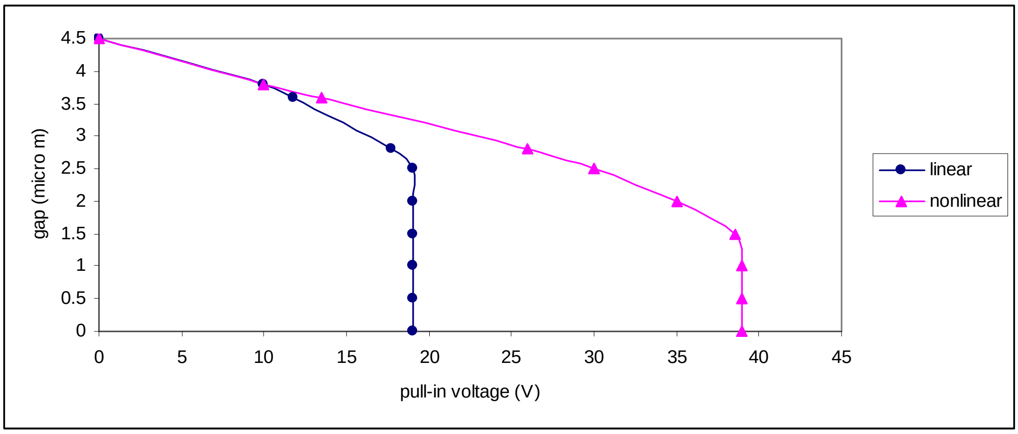

Fig.4. Comparison of linear and nonlinear geometry model results for a fixed-fixed beam with a gap 4.5 μm .

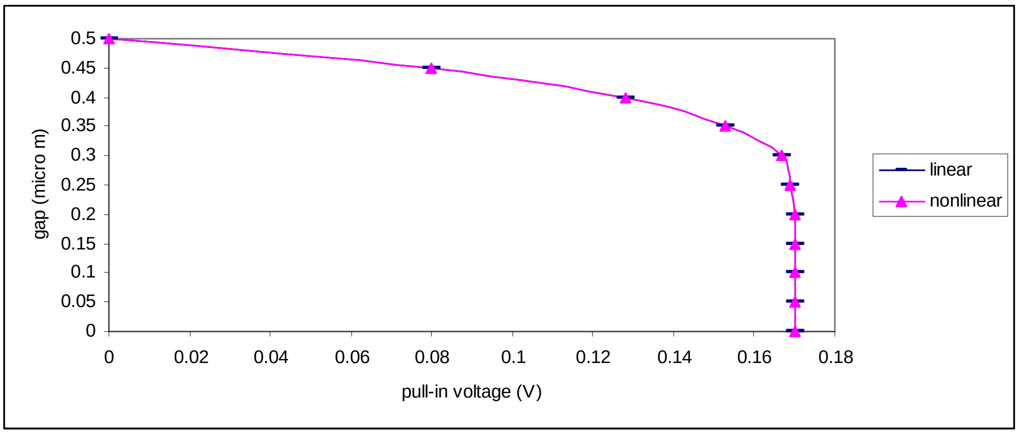

Fig.5. Comparison of linear and nonlinear geometry model results for a fixed-free beam with a gap 0.5 μm

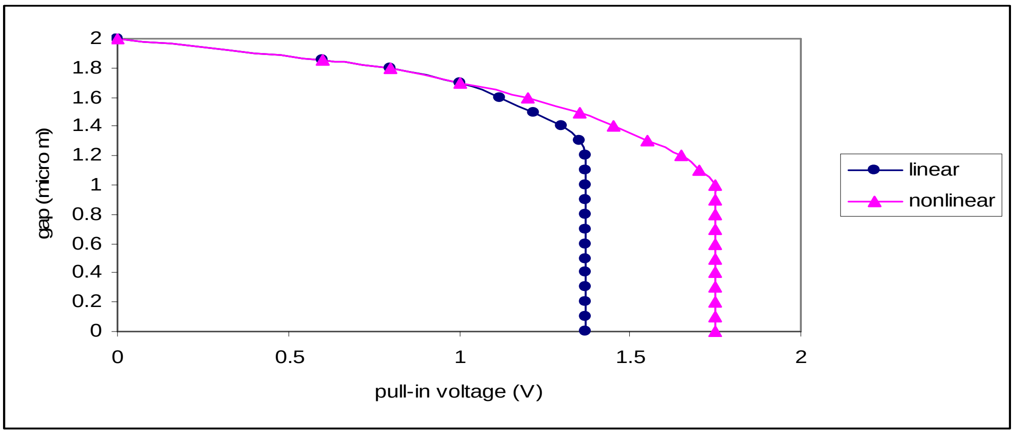

Fig.6. Comparison of linear and nonlinear geometry model results for a fixed-free beam with a gap 2 μm .

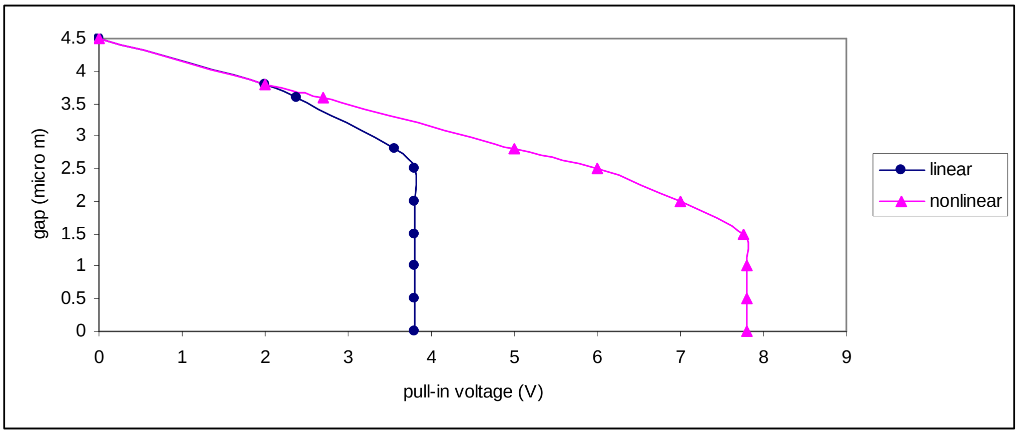

Fig.7. Comparison of linear and nonlinear geometry model results for a fixed-free beam with a gap 4.5 μm .

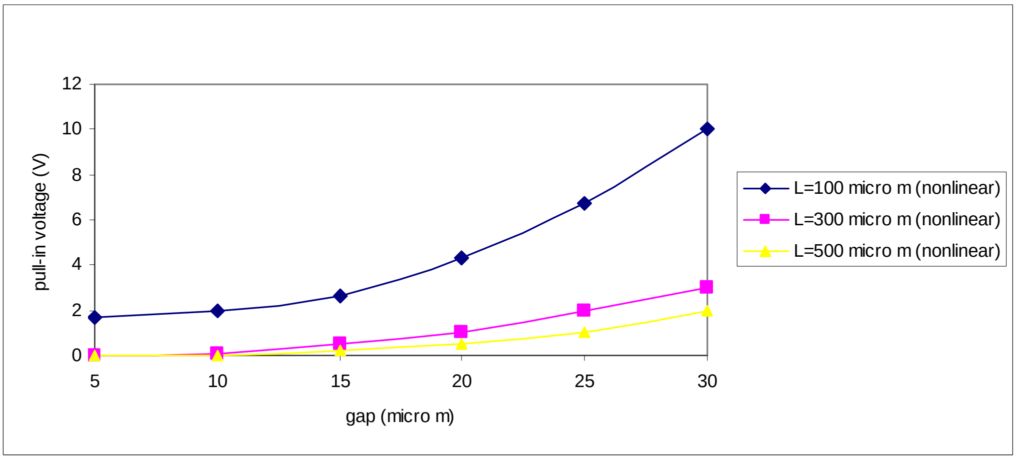

Fig.8. Gap vs. pull-in voltage for cantilever beams with a thickness of 1 μm . For length=100 μm , the difference in pull-in voltage between linear and nonlinear geometry model is significant when the gap is larger than 15 μm . For a length larger than 350 μm , the pull-in voltages obtained with linear and nonlinear geometry model are identical.

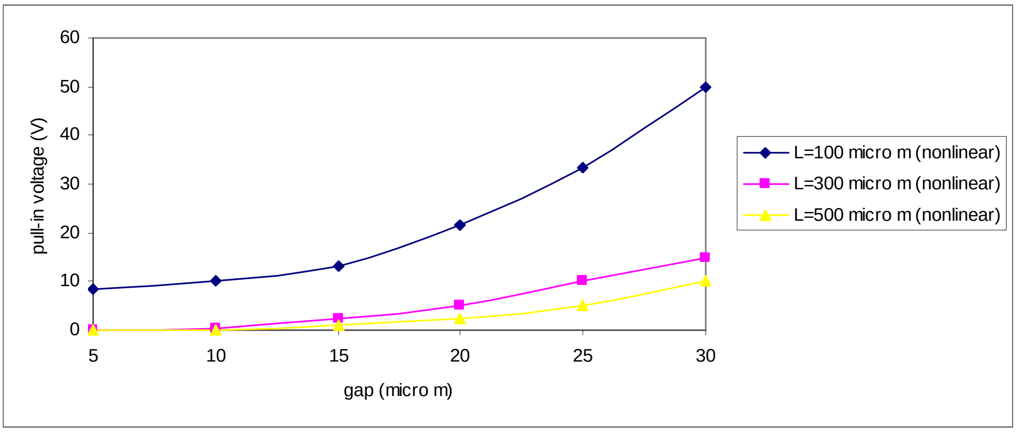

Fig.9. Gap vs. pull-in voltage for cantilever beams with a thickness of 4 μm . For length=100 μm , the difference in pull-in voltage between linear and nonlinear geometry model is significant when the gap is larger than 15 μm . For a length larger than 350 μm , the pull-in voltages obtained with linear and nonlinear geometry model are identical.

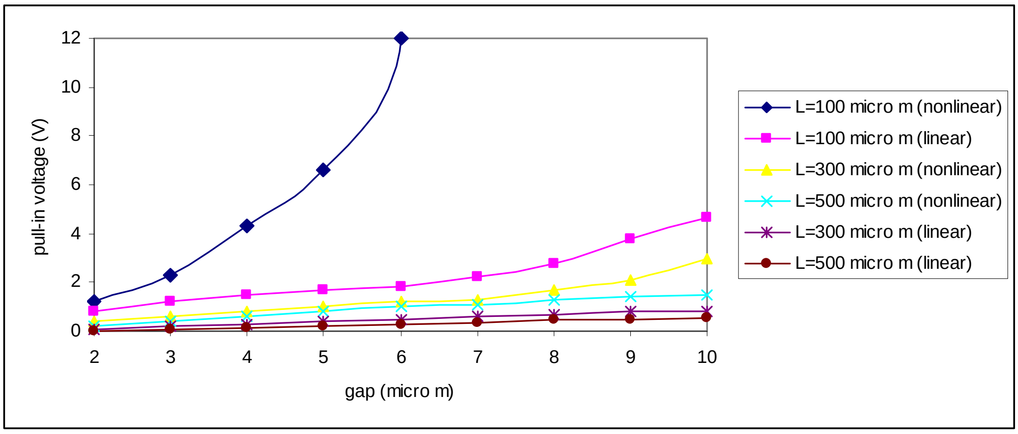

Fig.10. Gap vs. pull-in voltage for fixed-fixed beams with a thickness of 0.5 μm . Observe the large difference in pull-in voltage obtained from linear and nonlinear geometry model of beam.

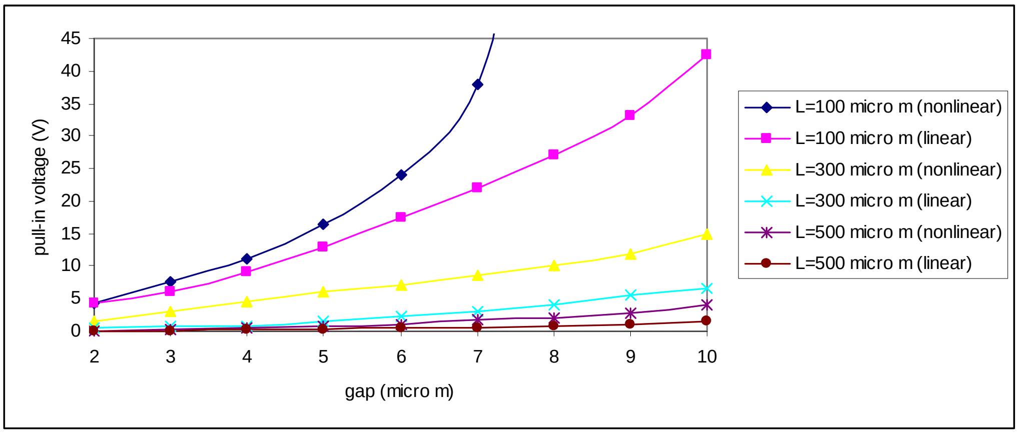

Fig.11. Gap vs. pull-in voltage for fixed-fixed beams with a thickness of 2 μm .

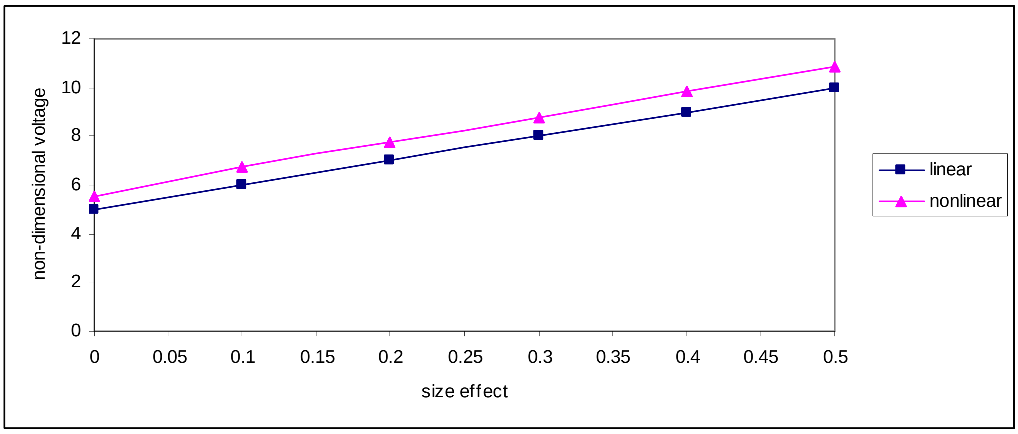

Fig.12. Pull-in voltage vs. size effect for fixed-fixed beam with gap 2.5 μm, a thickness of 1 μm, length 300 μm and width 0.5 μm, for nonlinear geometry model.

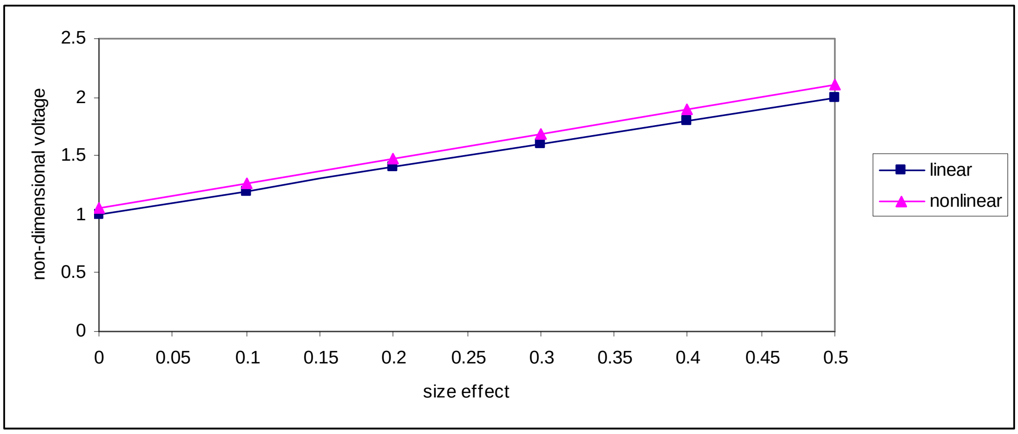

Fig.13. Pull-in voltage vs. size effect for cantilever beam with gap 2.5 μm, a thickness of 1 μm, length 300 μm and width 0.5 μm, for linear and nonlinear geometry model.

5. Conclusions

The primary contributions of the paper are summarized as follows.

1. For cantilever beams, length has a significant effect on the error in pull-in voltages, while for fixed-fixed beams, the length has little effect on the error. On the other hand, for fixed-fixed beams, thickness has significant effect on the error in pull-in voltage, while for cantilever beams it has little effect.
2. The static pull-in instability voltage of clamped–clamped and cantilever beam are compared. For both clamped–clamped and cantilever beams, the pull-in voltage in nonlinear geometry beam model is bigger than linear model.
3. For both fixed-fixed and cantilever beams by increasing of gap length, the pull-in voltage is significantly increased.
4. For both fixed-fixed and cantilever beams by increasing of thickness of beams, the pull-in voltage is significantly increased.

5. For both fixed-fixed and cantilever beams by increasing of length of beams, the pull-in voltage is significantly decreased.
6. By using modified couple stress theory, it is found that the dimensionless pull-in voltage of MEMS increases linearly due to the size effect. This emphasizes the importance of size effect consideration in design and analysis of MEMS.
The conclusion above indicates that the geometry of beam has significant influences on the electro-static characteristics of micro-beams that can be designed to tailor for the desired performance in different MEMS applications.

References

[1] Khatami, I., Pashai, M.H., Tolou, N., Comparative vibration analysis of a parametrically nonlinear excited oscillator using HPM and numerical method, *Mathematical Problems in Engineering*, doi:10.1155/2008/956170.

[2] Gasparini, A.M., Saetta, A.V., Vitaliani, R.V., on the stability and instability regions of non-conservative continuous system under partially follower forces, *Comput. Meth. Appl. Mech. Eng.*, 124 (1-2), 63-78, 1995.

[3] Osterberg, P.M., Senturia, S.D., M-TEST: A test chip for MEMS material property measurements using electrostatically actuated test structures, *J. Microelectromech. Syst*., 6 (2), 107-118, 1997.

[4] Osterberg, P.M., Gupta, R.K., Gilbert, J.R., Senturia, S.D., Quantitative models for the measurement of residual stress, poisson ratio and young's modulus using electrostatic pull-in of beams and diaphragms, *Proceedings of the Solid- State Sensor and Actuator Workshop, Hilton Head, SC*, 1994.

[5] Sadeghian, H., Rezazadeh, G., Osterberg, P., Application of the generalized differential quadrature method to the study of pull-in phenomena of MEMS switches, *IEEE/ASME J. Micro Electro Mech. Sys*., 16 (6), 1334-1340, 2007.

[6] Salekdeh, Y.A., Koochi, A., Beni, Y.T., Abadyan, M., Modeling effect of three nano-scale physical phenomena on instability voltage of multi-layer MEMS/NEMS: Material size dependency, van der waals force and non-classic support conditions, *Trends in Applied Sciences Research*, 7(1), 1-17, 2012.

[7] Batra, R.C., Porfiri, M., Spinello, D., Review of modeling electrostatically actuated microelectromechanical systems, *Smart Mater. Struct*., 16, R23-R31, 2007.

[8] Lin, W.H., Zhao, Y.P., Pull-in instability of micro-switch actuators: Model review, *Int. J. Nonlinear Sci. Numer. Simulation*, 9 (2), 175-184, 2008.

[9] Koiter, W.T., Couple-stresses in the theory of elasticity: I and II. *Proceedings of the Koninklijke Nederlandse Akademie van Wetenschappen Series B*, 6717-6744, 1964.

[10] Mindlin, R.D., Tiersten, H.F., Effects of couple-stresses in linear elasticity, *Archive for Rational Mechanics and Analysis*, 11(1), 415-448, 1962.

[11] Toupin, R.A., Elastic materials with couple-stresses, *Archive for Rational Mechanics and Analysis*, 11(1), 385–414, 1962.

[12] Anthoine, A., Effect of couple-stresses on the elastic bending of beams, *International Journal of Solids and Structures*, 37, 1003-1018, 2000.

[13] Yang, F., Chong, A.C. M., Lam, D.C.C., Tong, P., Couple stress based strain gradient theory for elasticity, *International Journal of Solids and Structures*, 39(10), 2731-2743, 2002.

[14] Xia, W., Wang, L., Yin, L., Nonlinear non-classical microscale beams: Static bending, postbuckling and free vibration, *International Journal of Engineering Science*, 48, 2044-2053, 2010.
[15] Asghari, M., Rahaeifard, M., Kahrobaiyan, M.H., Ahmadian, M.T., on the size-dependent behavior of functionally graded micro-beams, *Materials and Design*, 32, 1435-1443, 2011.
[16] Rong, H., Huang, Q.A., Nie, M., Li, W., An analytical model for pull-in voltage of clamped–clamped multilayer beams, *Sens. Actuators A*, 116, 15-21, 2004.
[17] Yang, F., Chong, A.C.M., Lam, D.C.C., Tong, P., Couple stress based strain gradient theory for elasticity, *International Journal of Solids and Structures*, 39 (10), 2731-2743, 2002.
[18] Shengli, K., Shenjie, Z., Zhifeng, N., Kai, W., The size-dependent natural frequency of Bernoulli–Euler micro-beams, *Journal of Engineering Science*, 46, 427-437, 2008.
[19] Ma, H.M., Gao, X.L., Reddy, J.N., A microstructure-dependent Timoshenko beam model based on a modified couple stress theory, *Journal of the Mechanics and Physics of Solids*, 56, 3379–3391, 2008.
[20] Gupta, R.K., Electrostatic pull-in test structure design for in-situ mechanical property measurements of microelectromechanical systems, Ph.D. Disserta-tion, Massachusetts Institute of Technology (MIT), Cambridge, MA., 1997.
[21] Zhao, J., Zhou, S., Wanga, B., Wang, X., Nonlinear microbeam model based on strain gradient theory, *Applied Mathematical Modelling*, 36, 2674-2686, 2012.